applied sciences

MDPI

Review

The Seismic Behavior of Rectangular Concrete-Encased Steel Bridge Piers: A Review

Mohammadreza Moradian and Munzer Hassan *

Department of Construction Engineering, École de Technologie Supérieure, University of Quebec, Montreal, QC H3C 1K3, Canada; mohammadreza.moradian.1@ens.etsmtl.ca
* Correspondence: munzer.hassan@etsmtl.ca

Abstract: This paper proposes a review of the previous research work and the representative publications regarding the seismic behavior of the concrete-encased steel (CES) columns. Concrete-encased steel sections are composed of steel sections encased in reinforced concrete members. The research work recently showed increased attention to this type of column due to its advantages compared to conventional reinforced concrete columns. Firstly, the analytical studies of the behavior of the CES columns under axial loads, including comparative studies between different research works, are presented. Then, the behavior of the CES columns under combined axial and flexural loads is also highlighted. An overview of the analytical confinement material models is addressed. In addition, the discussion and summary of the seismic behavior of the CES columns and the important parameters affecting the seismic behavior of these types of columns are included. Although important progress has been made by the previous studies in the CES columns under the axial load and the combination of axial and seismic loads, they fundamentally focused on the building columns, and little attention was paid to the impact of lateral reinforcement and their configuration in bridge piers. Due to the lack of studies on the parameters affecting the seismic behavior of the bridges, more studies should still be made to better understand the behavior of the CES bridge piers. This paper provides a reference for the research and engineering practice of concrete-encased steel bridge piers. It also concludes with suggestions for future studies to integrate the seismic requirement of the CES bridge piers in Canada.

Keywords: bridge seismic behavior; concrete-encased steel pier; ductility; confined concrete; plastic hinge; failure mode

Citation: Moradian, M.; Hassan, M. The Seismic Behavior of Rectangular Concrete-Encased Steel Bridge Piers: A Review. *Appl. Sci.* **2024**, *14*, 6627. https://doi.org/10.3390/app14156627

Academic Editor: Sang-Hyo Kim

Received: 16 June 2024
Revised: 14 July 2024
Accepted: 23 July 2024
Published: 29 July 2024

1. Introduction

Engineers have traditionally employed structural components made of steel forms combined with either plain or reinforced concrete. Earlier constructions only focused on the fire and corrosion resistance that the concrete provided for the steel shapes. However, studies on the strength of these members were carried out in the early 1900s, and by 1924, design guidelines had been developed. With the introduction of contemporary composite frame construction in tall structures in recent years, engineers have proposed innovative and practical ways to increase the resistance and ductility of concrete and steel reinforcement bars by using steel sections encased in concrete, also known as concrete-encased steel (CES) sections [1].

The use of concrete-encased columns in structures can reduce the size of the columns and reduce construction costs. In addition, its corrosion and fire resistance are both highly improved. Compared to ordinary columns, steel columns encased in concrete have substantially fewer long-term failures. It has been demonstrated that the ultimate axial load capacity of the CES columns is higher than a reinforced concrete column. This means that the structural steel improved the ultimate load resistance of the CES column [2]. Furthermore, an analytical and experimental study reveals that the axially loaded CES columns can sustain higher axial loads and undergo a smaller axial deformation compared

to a conventional reinforced concrete column [3]. The steel and concrete composite building technology combines the flexibility and stiffness of reinforced concrete with the assistance of reinforcing bars to create a cost-effective structure. Generally speaking, the idea that two or more components are combined to make an efficient structure is what gives composite buildings their strength [4]. Nevertheless, the CES columns have certain limitations too. In some cases, it is difficult to cast the concrete since the steel ratio is high and the space between the steel section and the rebars makes it difficult to pour the concrete. During the design phase, the engineers must be extremely mindful of any potential issues with the positioning of the reinforcing steel and congestion as they impact the pier's constructability, just like with any other concrete column with reinforcing steel [1]. Furthermore, the initial cost of construction of a CES column could be higher than a conventional reinforced concrete column. However, the increase in durability of the CES columns can justify a higher initial cost.

Major infrastructure, including railroads and bridges, ought to be built to withstand significant seismic ground motion. In the CES columns, integrated concrete and steel profile sections help to obtain a high load-carrying capacity and high ductility. Figure 1 presents an example of a recent bridge construction using concrete-encased steel columns in China in 2024 [5].

Figure 1. Tian'e Longtan Bridge constructed using CES columns, reprinted with permission from [5], 2024, www.highestbridges.com, accessed on 15 June 2024.

The application of the CES column in buildings is more frequent than in bridges. Most applications on bridges until now have been on the steel–concrete composite high bridge piers. More specifically, in the mountainous regions, where large quantities of rebars are required as well as concentrated stirrups are required for a conventional reinforced concrete column. In addition, a large number of stirrups and reinforcing bars lowers the quality of construction and reduces efficiency while also making construction more challenging.

As illustrated in Figure 2, hybrid hollow high piers, which are a form of CES columns, offer a new approach to reducing the excessive use of steel bars in traditional bridge piers. A portion of the axial direct reinforcing bars installed using the conventional method are replaced by structural steel and stirrups or spiral reinforcement. When compared to typical reinforced concrete piers, the hybrid hollow high pier has a number of advantages, including increased earthquake resistance, increased economy and efficiency during construction, improved quality and aesthetics, and the preservation of the environment [6].

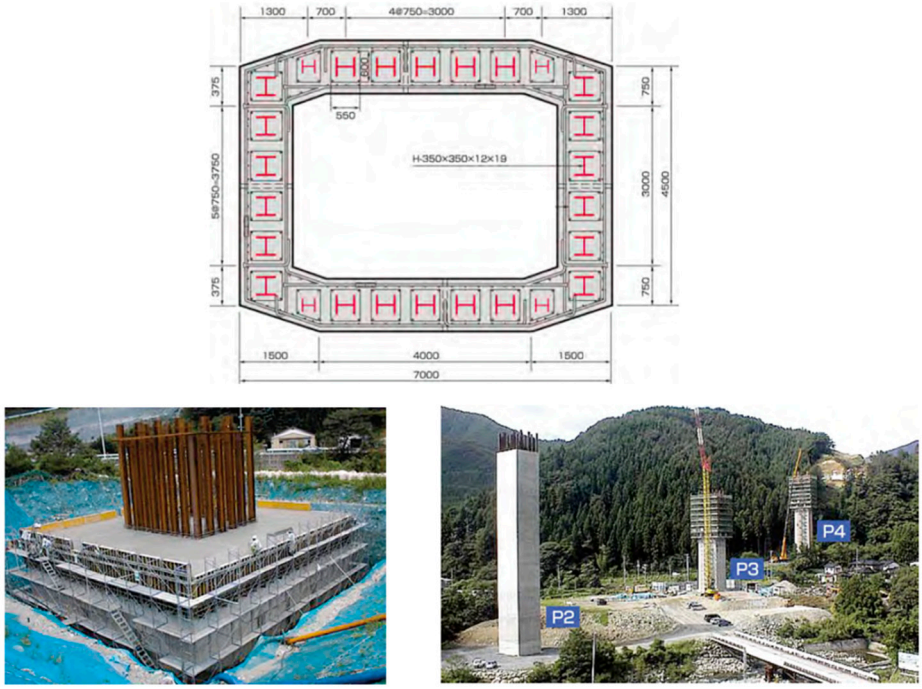

Figure 2. Hybrid hollow high pier of bridge constructed using CES concept; dimensions are in millimeters; reprinted with permission from [7], 2018, www.actec.or.jp.

In the context of the Canadian weather, the CES piers help to increase the durability of the bridges in harsh winter environments. Increasing the durability of the infrastructure becomes one of the most important aspects of the bridge design in view of its large impact on the economy. Reinforcement corrosion directly causes concrete deterioration, specifically in the bridge piers. In order to melt down the ice on the roads, the de-icing salts are spread out on the road during the winter. However, most bridge piers that are near the roads are in the splash zone of the mix of de-icing salt and the melting water caused by passing vehicles. Once the water is absorbed and combined with chloride ions, the corrosion process on the reinforcement rebars begins [8]. With the corrosion of the reinforcement rebars, the expansion causes concrete cover spalling, the reinforcement rebars become more exposed to the watery de-icing salt, and the corrosion process accelerates quickly, causing a significant reduction in the reinforcement and therefore leading to a load capacity reduction of the bridge. In CES piers, since the steel profile is in the center of the column, the possibility of the penetration of the de-icing salt to the steel profile reduces considerably. However, the reinforcing rebars are still exposed, but the risk is less since the central steel profile can carry the vertical load without the contribution of the reinforcing rebars. Thus, the use of CES piers can improve the impact on the traffic during the repair works. In the case of conventional reinforced concrete columns, the repair of the corroded rebars causes a bridge closure, either partially or completely because of the reduction in the capacity of the column during the repair works. However, using the CES piers can allow us to keep the bridge open during the repair of the corroded rebars since the steel profile can assure the capacity of the bridge for the service load.

The CES column has great potential to be widely used in future construction as engineering constructions evolve toward high-rise buildings, heavy-loading structures, and large-span bridges. Given the lack of well-developed Canadian design code specifications, it is crucial to compile the body of knowledge describing the behavior of the CES columns in order to facilitate the codification of the design guide.

This paper aims to present a thorough analysis of different CES column configurations, emphasizing their axial, flexural, and seismic performance as well as analytical modeling techniques. The main objective of this review is to present a thorough, insightful, and

useful overview of the field of bridge engineering, with a special emphasis on the concrete-encased steel (CES) column pier section. The goal of this study is to be a useful resource by illuminating the subtleties and complexity of different CES section calculations in bridge performance and analysis.

There are four main sections to this paper. The CES column configuration and their analysis methods are covered in Sections 2 and 3 respectively. The axial and flexural behavior of the CES columns is shown in the Section 4. The seismic and cyclic performance of the CES columns is reviewed in the Section 5, and recommendations for further research are offered in Section 6.

2. Typical Configuration of Concrete-Encased Steel Columns

A concrete-encased column has a concrete-covered steel specimen inside of it. The steel specimen's buckling behavior is improved, and its strength is further increased by the concrete surrounding it. One significant benefit of this encasement is its ability to prevent corrosion and fire.

Some of the typical configurations of the CES columns are presented in Figure 3. It should be noted that the configuration of the steel section, rebar ratio, and transversal reinforcement have an impact on the resistance and the ductility of the CES column.

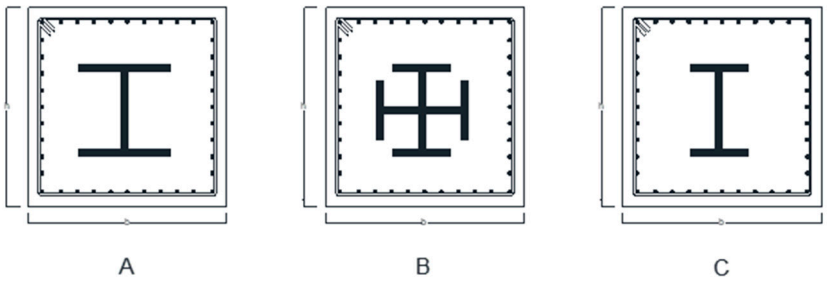

Figure 3. Typical cross section of CES columns. (**A**) H shape section, (**B**) Combined I shape section, (**C**) I shape section.

The CES sections are not presented in the Canadian bridge design code CSA-S6 [9]. However, the American Concrete Institute code ACI 318-8 [10] prescribes that the cross-sectional area of the steel should be at least 1% of the total cross-sectional area. Also, the cross-sectional area of the steel should not exceed 8% of the total cross-sectional area [10]. According to the AISC 360-22 [11] the cross-sectional area of the steel profile should be at least 1% of the total cross-sectional area, and the minimum reinforcement ratio of the longitudinal rebars should be 0.4% of the total cross section.

Since there is no requirement to be found in the Canadian bridge design code CSA-S6 [9] regarding the CES sections, the requirements of the American Institute of Steel Construction code AISC 360-22 [11] are presented in this paper. According to the AISC 360-22, concrete shall have a specified compressive strength, f_c', of not less than 21 MPa nor more than 69 MPa for normal-weight concrete. The specified minimum yield stress of structural steel and the reinforcing rebars used in calculating the strength shall not exceed 525 MPa and 550 MPa, respectively [11].

3. Simulating the Behavior of the Concrete-Encased Steel Columns

For different configurations of the CES columns, the resistance of the confined concrete can be defined accordingly. Moreover, an extensive amount of research has been conducted to gather information regarding past research work on analytical models that consider the effect of confinement and other factors into account in order to simulate the actual mechanism of the CES columns [12].

The CES columns were analyzed using the fiber section model. The section is divided up into "n" fibers, which are not necessarily all of identical sizes. The stresses are integrated into the cross-sectional area in order to determine the straining actions, such as moment or

force. Each steel reinforcing bar, structural steel section, or concrete fiber has a specific set of material properties. Fiber stresses are calculated from them using the "plane sections remain plane" theory along with relevant constitutive models. There are several formulas for calculating the strain on the fiber as the loads increase. The section axial strain and curvatures with respect to a fixed reference system were described and they did not have to monitor the evolution of the neutral axis (NA) position [13].

Additionally, the impact of the load on the position of the natural axis (NA) was studied [14]. In order to calculate the stresses of the fibers and modules of elasticity, it should determine a constative model for uniaxial models for steel and concrete including the confinement effect. It was discovered that during an increase in the load, the CES column provided its initial strength against lateral shear. It should be noted that the initial stiffness in the model equations should be considered adequately [15–18].

The impact of flange shear studs for increasing stiffness and bending strength, the concrete's compressive strength, the mechanism of shear resistance of the CES section, and the necessary confinement level to provide appropriate ductility under seismic loading were all explored [16].

In order to account for the confinement impact on the CES columns made of cross-shaped steel and to predict the analytical axial load–displacement relationships of the columns [19,20], we adapted Mander's model. The structural steel segment increases the confining stress in the concrete zone. The confinement regions can be made simpler by transforming the parabolic sections, presented in Figure 4, into rectangular regions [21]. By considering the effect of unstiffened elements of the steel section on the confinement, one-half of the corresponding steel area is taken to calculate the confining stress [22].

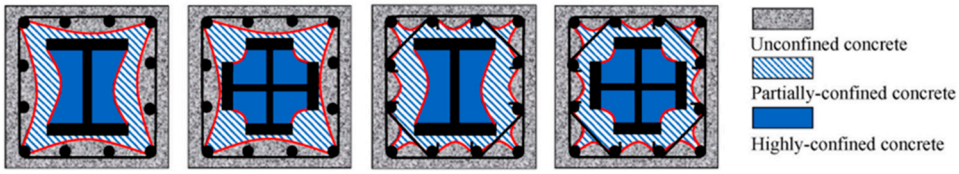

Figure 4. Definition of confinement of CES columns, reprinted with permission from [23], 2023, *Journal of Building Engineering*.

As presented in Figure 4, the concrete section in the CES column's cross section is divided into three sections, unconfined concrete (UC), partially confined concrete (PC), and highly confined concrete (HC). The stress–strain curves for the concrete are presented in Figure 5a. The steel section is also divided into three sections, the steel flange and the steel web as presented in Figure 5b, and the longitudinal reinforcement as presented in Figure 5c. Consequently, six distinct uniaxial stress–strain relationships are presented in this section [19].

Due to the steel flanges' bending stiffness, the steel section of the CES column could contribute to the expanded concrete's lateral confining pressure. The Mander model, first introduced for reinforced concrete [16], can be applied to HC in CES columns as long as it is established that the steel section's effective lateral confining pressure exists. Consequently, by closely examining the lateral interaction between the concrete and steel section, a unified stress–strain relation is provided for HC.

Based on the Mander model, the stress–strain relationship for PC is established. The Mander model predicts that hoops will yield at the maximum strain of confined concrete, but other experimental research work showed that high-strength hoops might not yield when the confinement effect is minimal [24]. As a result, modifications are required to determine the real stress in hoops. Therefore, it is imperative to ascertain the real stress status of the hoops, and the iterative process was used in this instance [25].

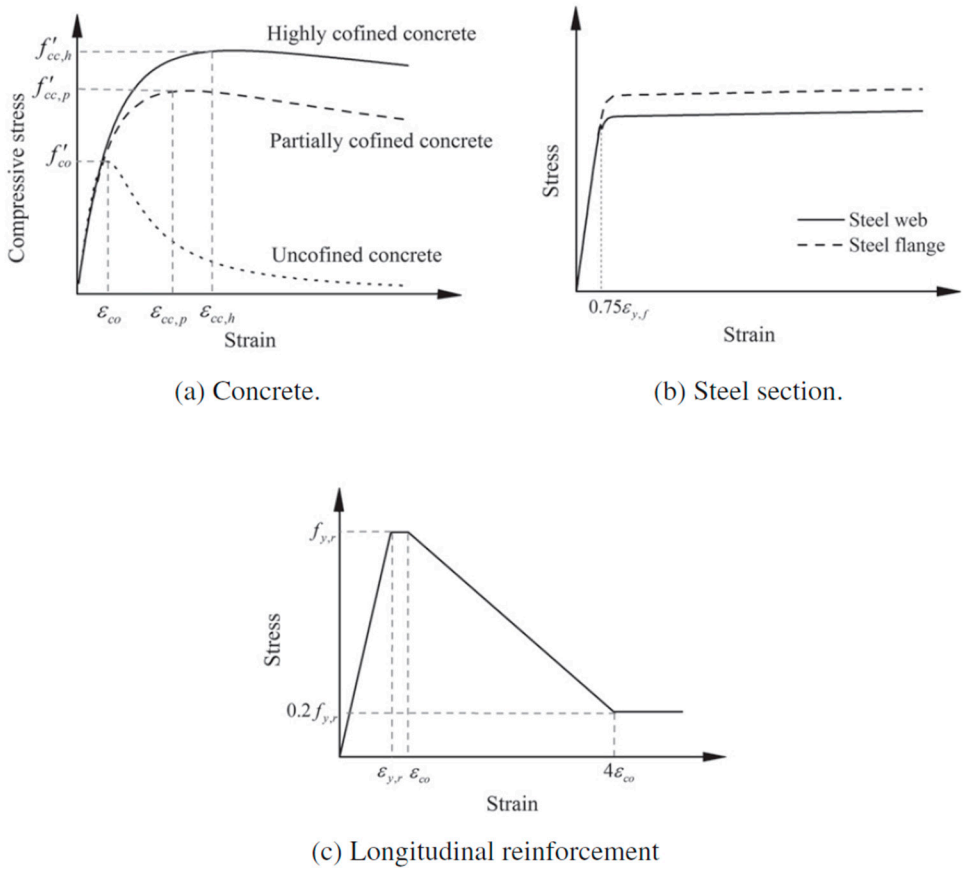

Figure 5. Stress–strain relationship of materials in CES section, reprinted with permission from [18], 2015, *Journal of Constructional Steel Research*.

It should be noted that the parameters that can impact the resistance of the confined concrete are the distribution of the longitudinal reinforcing bar, the volumetric ratio of the lateral reinforcement, and the spacing of the stirrups [16]. A reduction in the stirrup spacing enhances the post-peak behavior of the axial load–deformation behavior.

Furthermore, in order to investigate the confinement impact for highly and partially confined concrete, the confinement factors (K_p and K_h) have been suggested [22]. The concrete strength f'_{cc} for partially and highly confined concrete is described as presented in Equations (1) and (2), respectively, while f'_{co} is the compressive strength of the unconfined concrete.

$$f'_{cc} = K_p.f'_{co} \quad (1)$$

$$f'_{cc} = K_h.f'_{co} \quad (2)$$

The relations of the tie spacing versus the confinement factor K_p for partially confined concrete for columns are shown in Figure 6 [22]. The effectiveness of confinement by lateral reinforcement can be shown in Figure 6. It can be concluded that reducing stirrup spacing increases the confinement factor K_p.

The form of the structural steel section, which applies confining stress to the core concrete, affects the confinement factor K_h for highly confined concrete. The steel profile form versus confinement factor K_h relations and their impact on the efficiency of confinement are displayed in Figure 7. The structural steel, especially the cross-shaped section, increases the confining effect. The explanation for the change is that in contrast to I- or H-shaped steel sections, which confine the concrete in just one direction, cross-shaped steel sections can produce confining pressure in both directions, resulting in a greater value of the confinement factor K_h [22].

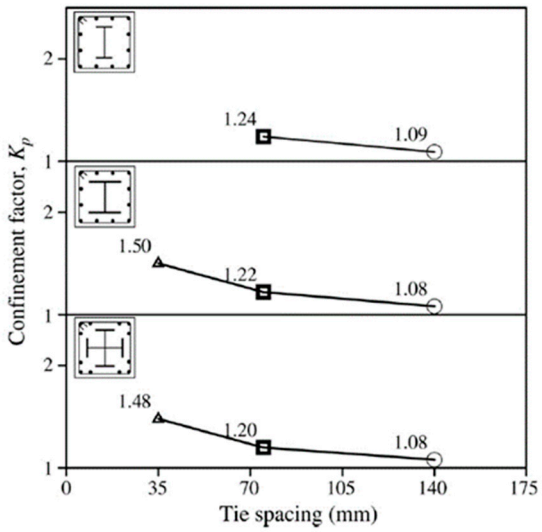

Figure 6. Confinement factor (k_p) for partially confined concrete, reprinted with permission from [22], 2006, *Journal of Constructional Steel Research*.

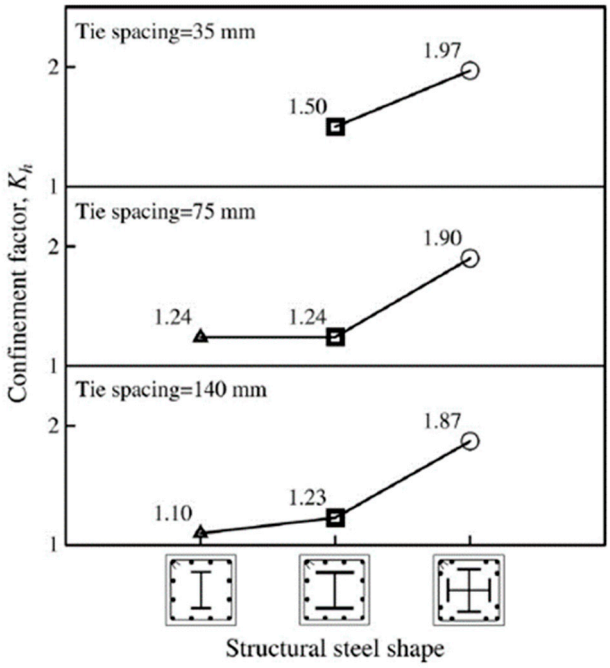

Figure 7. Confinement factor (K_h) for highly confined concrete, reprinted with permission from [22], 2006, *Journal of Constructional Steel Research*.

The effect of concrete confinement improves the ductility of CES columns but has little impact on the axial capacity since it activates after cover spalling. In addition, compared to shear-dominant CES columns, the flexural dominant CES columns benefit more from the confinement effect provided by stirrups [23].

Another research work has developed an analytical model to predict the axial compressive behavior of CES columns [19]. The confinement factors K_p and K_h for PC and HC, respectively, are described as follows:

$$k_p = -1.254 + 2.254\sqrt{1 + \frac{7.94 f'_{le,p}}{f'_{co}}} - 2\frac{f'_{le,p}}{f'_{co}} \quad (3)$$

$$k_h = -1.254 + 2.254\sqrt{1 + \frac{7.94 f'_{le,h}}{f'_{co}}} - 2\frac{f'_{le,h}}{f'_{co}} \tag{4}$$

As presented in Equation (3), $f'_{le,p}$ is the effective confining pressure from stirrups. It can be obtained as follows:

$$f'_{le,p} = \xi f_{rh} \tag{5}$$

where f_{rh} is the real stress in the stirrups, and ξ, is the confinement effectiveness factor for the partially confined concrete.

The confinement effectiveness factor for the partially confined concrete can be presented as

$$\xi = \frac{\left(1 - \frac{0.5 E_s \varepsilon_{co}}{f_{y,h}}\right) f'_{co}}{14 E_s \varepsilon_{co}} \tag{6}$$

The real stress in the stirrups f_{rh} can be obtained as follows:

$$f_{rh} = \frac{0.5\ E_s \varepsilon_{co}}{1 - 14\zeta} \tag{7}$$

where E_s is the elastic modulus for steel, ε_{co} is the peak strain of the unconfined concrete, and the ζ is the coefficient in the simplified method for partially confined concrete presented as follows:

$$\zeta = \frac{\xi E_s \varepsilon_{co}}{f'_{co}} \tag{8}$$

As presented in Equation (4), $f'_{le,h}$ is the effective lateral confining pressure for highly confined concrete. It can be obtained as follows:

$$f'_{le,h} = f'_{le,p} + f'_{le,s} \tag{9}$$

where $f'_{le,p}$ is the effective lateral confining pressure from stirrups presented previously in Equation (5), and $f'_{le,s}$ is the effective lateral confining pressure from the steel section presented as follows:

$$f'_{le,s} = k_{es} k_{ea} f'_{ls} \tag{10}$$

where k_{es} is the stress effectiveness coefficient considering the uneven distribution of confining pressure, k_{ea} is the confinement effectiveness coefficient considering different confining states in highly confined concrete, and $f'_{l,s}$ is the nominal confining pressure between highly confined concrete and steel sections in the CES column which can be obtained as follows:

$$f'_{l,s} = \frac{2}{3} q_u \tag{11}$$

where q_u is the maximum lateral pressure between the highly confined concrete and steel sections in the CES column presented as follows:

$$q_u = \frac{t_f^2}{4b^2} f_{y,f} \tag{12}$$

where t_f is the thickness of the steel flange, b is the cantilevered length of the steel flange, and $f_{y,f}$ is the yield strength of the steel flange.

The stress effectiveness coefficient in Equation (10) is given by

$$k_{es} = \frac{3\lambda}{2\lambda + 1} \tag{13}$$

where λ is the blocking ratio of the steel section presented as follows:

$$\lambda = \frac{b}{h} \tag{14}$$

where b is the cantilevered length of the steel flange, and h is the clear distance between two steel flanges in the steel I section.

The confinement effectiveness coefficient k_{ea} can be obtained as follows:

$$k_{ea} = \frac{1 - \frac{\pi}{4}\left(1 - \frac{\lambda}{3}\right)^2}{1 - \frac{1}{2}(1 - \lambda)^2} \tag{15}$$

In order to better understand the process of deriving the confinement factors (K_p and K_h), Figure 8 presents a flowchart process calculation.

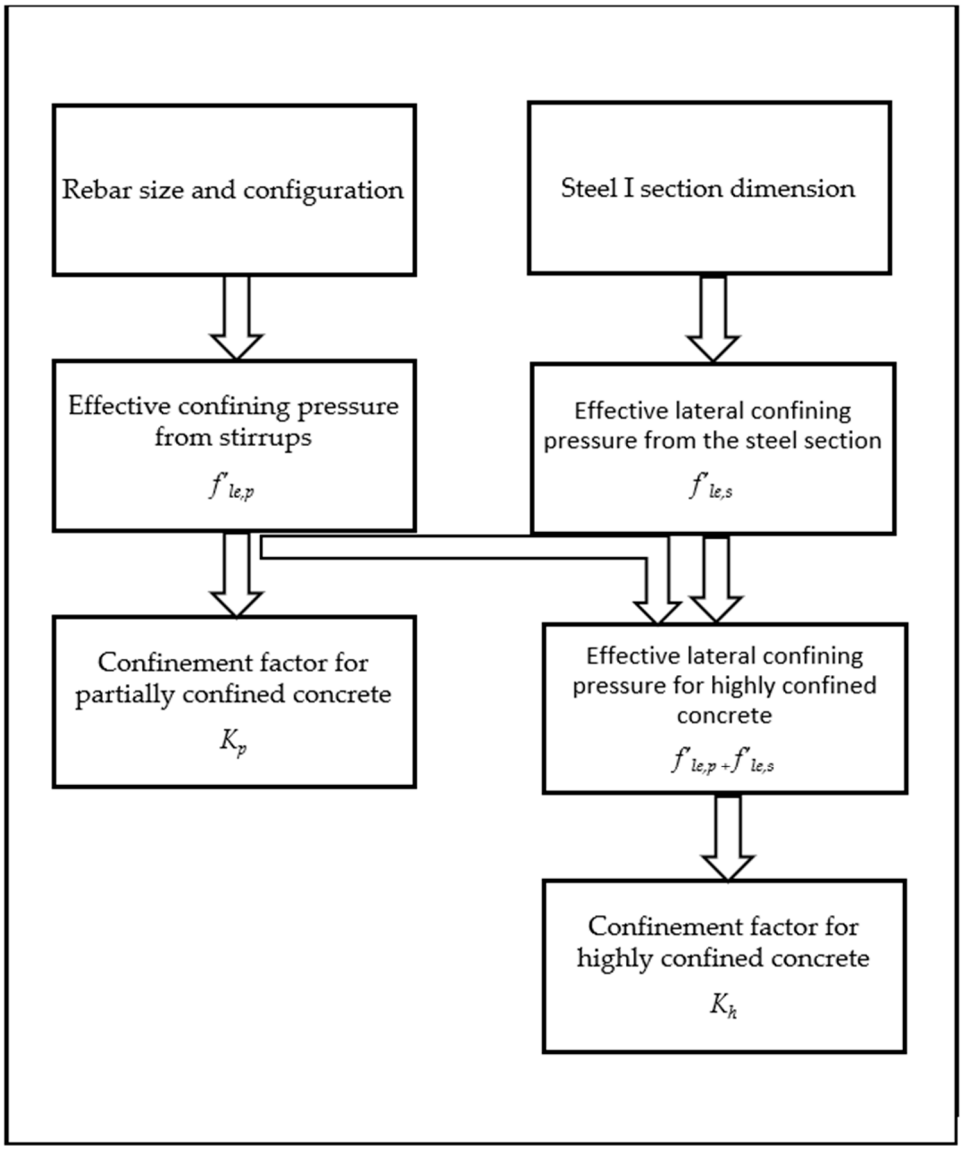

Figure 8. Confinement factor process flowchart.

In this section, two methods are reviewed in order to obtain the confinement factors for partially confined concrete and highly confined concrete (K_p and K_h). The first method presented by [22] is based on the shape of the steel section as well as the longitudinal distance between the stirrups while the second method is based on the shape and the dimension of the steel section as well as the stirrups [19]. The confinement factors calculated from both methods are comparable for a steel I section encased in a rectangular concrete section.

4. Axial–Flexural Behavior of Concrete-Encased Steel Columns

Since axial compression is an uncommon loading scheme in real construction, research on the behavior of the axial–flexural interaction is necessary because the CES bridge piers are typically subjected to a combination of axial force and bending moment. However, there are a few experimental investigations of the eccentric-compressed CES columns. The limited number of experimental investigations reveals the axial–flexural failure mechanism, and Figure 9 illustrates the common failure modes [26]. In other words, tension failure and compression failure are two distinct groups into which axial–flexural failure may fall. Important elements having an impact on the CES column axial behaviors include the concrete strength, the end eccentricity ratio, the slenderness ratio, the structural steel index, and the transverse reinforcement ratio [27].

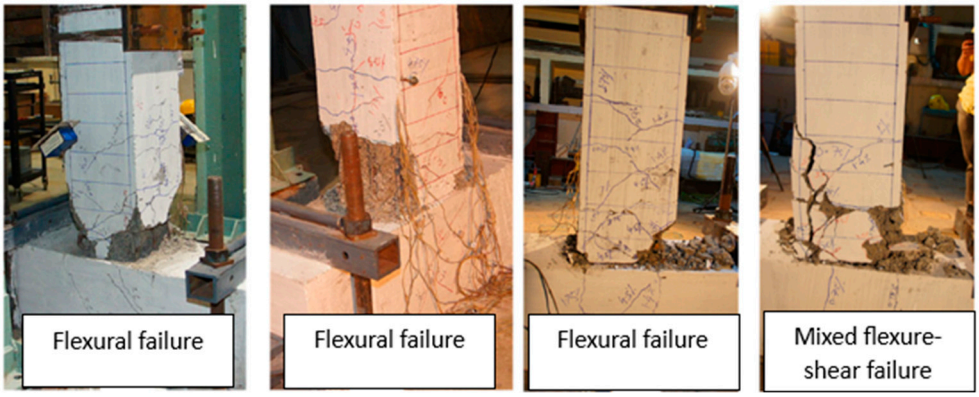

Figure 9. Failure mode for eccentrically loaded CES column, reprinted with permission from [28], 2021, *Journal of Building Engineering*.

Concrete cracking and the occurrence of the longitudinal bars' yield strength at the tension side are characteristics of tension failure, while concrete cover spalling and crushing, rebar buckling, and stirrup opening are features of compression failure. These are followed by the longitudinal rebar yielding at the tension side [29]. While some specimens experience the cover spalling phenomena, it is not as noticeable as it is in specimens that are concentrically compressed. This could be due to the concrete's enhanced deformability under flexural loading and its non-uniform compressive stress distribution [30]. It is possible to approximate the overall deflection along the height as a half sinusoidal wave, and as there is no visible bond slippage between the steel section and the concrete up until failure, the cross-section analysis can assume a flawless bond [31]. It appears that an increase in structural steel strength has minimal effect on the CES strength for columns that have higher relative slenderness ratios due to the flexural buckling failure mode [32].

Figure 10 presents the axial–flexural behavior of the CES column according to the Architectural Institute of Japan Standard [33].

Axial force–bending moment (N-M) interaction diagrams are typically utilized to illustrate the axial–flexural capacity of CES columns. These diagrams can be condensed into piece-wise diagrams to make calculations easier. The estimated bending moment capacity is decreased by a reduction coefficient in order to account for the potential non-attainment of the full plastic stress distribution. Figure 11 presents the axial–flexural diagram of a CES column according to [34]. Figure 11a presents the cross-section capacity of CES columns under external forces, through seven interaction diagrams from a 3D surface on the coordinate system. Figure 11b shows cutting of the 3D surface in a longitudinal direction while Figure 11c shows that cutting of the 3D surface in a latitudinal direction results in a bundle of curves [34].

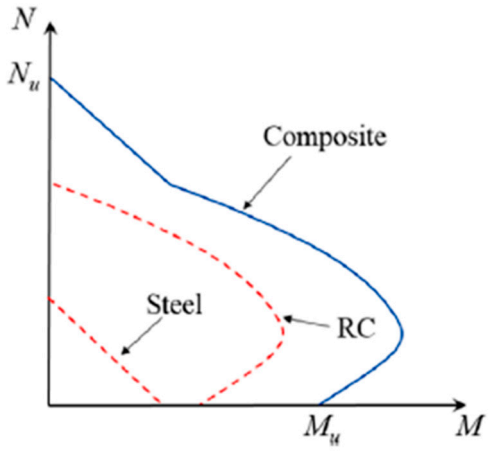

Figure 10. Axial–flexural behavior of CES column according to AIJ-2014 code [33], reprinted with permission from [30], 2019, *Construction and Building Materials*.

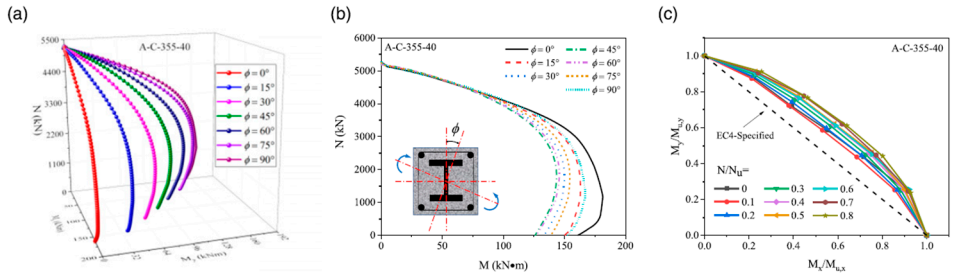

Figure 11. Three-dimensional N-M surface and 2D biaxial N-M curves obtained by fiber section analysis, (**a**) 3D interaction diagrams, (**b**) longitudinal direction cut from 3D interaction diagram, (**c**) latitudinal direction cut from 3D interaction diagram, reprinted with permission from [34], 2022, *Advances in Structural Engineering*.

Another important aspect of the design of the CES columns is the slenderness ration *(L/b)*. The Canadian bridge design code CSA-S6 [9] does not include CES section requirements. However, according to the British code BS.5400-5 [35], the slenderness range for columns *L/b* should be less than or equal to 30 [35].

5. Concrete-Encased Steel Column Behaviors under Cyclic Loads

In this section, a review of the recent study on the seismic and cyclic behavior of the CES columns is presented. In addition, the parameters that can have an impact on the seismic behavior of the CES columns, such as steel ratio, shear span ratio, axial load ratio, embedded depth ratio, steel shear connections, and concrete resistance are highlighted in detail.

A large amount of CES column test data are gathered and reviewed in this paper from a recent decade's worth of research. Based on material composition, this review does not include stainless steel, steel fiber-reinforced concrete, recycled aggregate concrete, ultra-high-performance concrete, or engineered cementitious composite because of differences in material properties.

The primary approaches applied to evaluate the seismic performance of CES columns in laboratory settings are low reversed cyclic loading and constant axial force. In order to simulate a seismic event, the CES column is first loaded axially to reach the target load ratio. After that, it is loaded horizontally with reversed displacement increments. An important performance indicator for evaluating energy dissipation capacity, load-bearing capacity, displacement ductility, stiffness degradation, capacity deterioration, etc., is the hysteresis curve (P-Δ). CES columns typically fail in flexural mode, shear–flexural mode, and shear mode, depending on the primary design parameters.

In seismically active regions, the CES column's exceptional seismic performance is important. Due to this particular advantage, a significant amount of the present review has been conducted to examine the seismic behavior of CES columns using quasi-static loading, in which the column top is subjected to a low reversed cyclic horizontal force and a required axial compressive force. The shear span ratio, axial load ratio, stirrup arrangement, confinement ratio, shear connectors, and material strengths are among the important factors that have an impact on the seismic behavior of the CES columns [12].

According to the research study, when using a sufficient amount of steel, CES column specimens have remarkable cyclic strength and ductility [26]. CES column specimens, in particular, have a high load-bearing capability even after longitudinal bar buckling and spalling of the concrete cover. Based on these tests, the ultimate state and the restorable limit state were determined to be local buckling of the H-shaped steel followed by spalling of the concrete cover.

The seismic behavior of 26 steel concrete composite columns under low cyclic reversed loading has been studied [36]. According to this study, under seismic load, the steel–concrete composite columns exhibit a bending failure mechanism. The deformation capacity is great, and the strength depreciation is modest. It demonstrates that the composite steel–concrete members have advantageous seismic behavior. As presented in Figure 12, all of the studied samples showed signs of bending failure, and the failure mechanism followed the standard procedures for bending failure members.

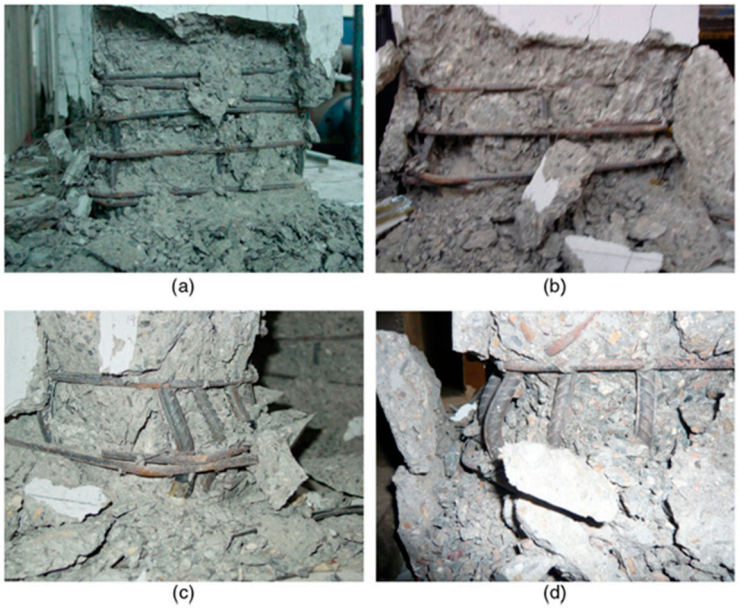

Figure 12. Flexural failure of the four studied specimens, (**a**,**b**) cover spalling, (**c**,**d**) reinforcement buckling, reprinted with permission from [36], 2014, *Journal of Structural Engineering*.

Five CES columns that were designed to collapse in flexural tension or flexural compression have had their cyclic behavior examined experimentally by [37]. According to current seismic evaluation rules, CES columns with non-seismic detail and low axial loads controlled by flexural tension appear to meet the acceptance criteria. However, the high axial loads controlled by flexural compression and the lack of seismic details in CES columns make them deficient for current seismic assessment acceptance standards [37]. These results show that the presence of the steel section in the concrete column helps to improve the seismic behavior of the CES column even with no additional seismic consideration for the rebars and the stirrups.

It appears that one of the key elements impacting the seismic performance of CES columns is the shear span ratio. While numerous elements influence the damage pattern collectively, an increase in span ratio tends to shift the damage from a shear-dominant

failure to a bending-dominant failure. The outcome shows that the shear span ratio and the slenderness ratio have a significant impact on the behavior of CES columns. According to [38], ductility increased, and the failure process slowed down as the ratio of shear span increased. The long columns' carrying capacity decreased as the ratio of slenderness increased, yet the chance of an abrupt collapse increased [39].

Table 1 summarizes some related previous research regarding the seismic behavior of the concrete-encased steel bridge piers. It shows the name of the authors, the year of the study, the type, and the achievement of analysis.

Table 1. Summary of some related previous research.

Author	Type of Analysis	Achievement of Analysis
Hassan et al., 2021 [37]	Seismic performance of steel-reinforced concrete composite columns	CES columns with non-seismic detail and low axial loads controlled by flexural tension appear to meet the acceptance criteria
Dong et al., 2021 [40]	Seismic behavior of large-size encased cross-section steel-reinforced columns	The influence of the steel ratio is more significant under a low axial load ratio
Naito et al., 2011 [26]	Ductility evaluation of concrete-encased steel bridge piers	When using a sufficient amount of steel, CES columns have remarkable cyclic strength and ductility
Chen et al., 2014 [36]	Study on seismic behavior of fully encased steel–concrete composite columns	Under seismic load, the steel–concrete composite columns exhibit a bending failure mechanism
Yang and Li, 2012 [39]	Study on behaviors of steel-reinforced concrete columns	The long columns' carrying capacity decreased as the ratio of slenderness increased
Zhang et al., 2012 [38]	Flexural behavior of SRC columns under axial and bilateral loading	The axial load ratio was the most influencing factor on the ductility of columns
Zhu et al., 2016 [41]	Experimental study on steel reinforced concrete columns under cyclic lateral force	The axial compression ratio has an impact on the deformation capacity and the energy dissipation capacity
Zhang et al., 2019 [6]	Study on ultimate load and ductility of concrete-encased steel composite columns	A larger load ratio is shown to reduce energy dissipation and deformation capacities

One of the other most important factors affecting the cyclic behavior of the CES columns is the axial load ratio. Many researchers have examined the impact of this parameter. The capacity of energy dissipation, ductility, carrying capacity, stiffness degradation, and axial load distribution on the column are all impacted by the axial load ratio. A significant influence on the hysteresis behavior was the ratio of the applied axial compressive load [12]. Because of a significant increase in the moment of secondary bending caused by the axial loads, the columns appeared to have less capacity for energy dissipation and displacement ductility when the applied axial load was 40% of the ultimate load, as opposed to the columns with 20% of the axial ultimate load [22]. The carrying capacity, damage pattern, and deformation ability of the high-resistance CES columns are all impacted by the axial load ratio. The axial load ratio was the most influencing factor on the ductility of columns [38]. The axial compression ratio has an impact on the seismic resistance behavior of CES columns with high-strength concrete [39]. This has a detrimental influence on the deformation capacity and the energy dissipation capacity [41].

Furthermore, a larger load ratio is shown to reduce energy dissipation and deformation capacities [6]. However, a high load ratio increases the longitudinal reinforcing bars' dowel action and prevents the spread of oblique shear cracks, increasing the load-carrying capacity to some degree [41]. Regarding the impact of shear studs, it was found that while they improve the deformation capacity and lessen stiffness degradation, they do not affect the

seismic behavior preceding concrete cover spalling [41]. It has been demonstrated that a bigger steel section size results in superior ductility and less stiffness degradation when considering the steel area ratio. It was found that structural steel is more advantageous in the event of a big axial load [41], while another researcher notes that the influence of the steel ratio is more significant under a low axial load ratio [40].

One other factor that has an impact on the seismic behavior of the CES column is the embedded depth ratio. The steel section of the CES column is embedded in the foundation. This length is known as h_b. The height of the steel section is also known as the h_a. The ratio of the embedded length of the steel section to section height is known as the embedded depth ratio, and it presented as h_b/h_a.

To preserve the CES column's strength capability and seismic behavior, an appropriate steel embedding depth is needed [42]. Also, the steel-embedded depth ratio for the CES column subjected to monotonic loading has been studied, and it was found that 1.67 was a suitable value for an ordinary CES column [43]. However, it is recommended that the minimum steel embedded depth ratio for the CES columns should be a minimum of 2.5 in order to take safety precautions into account [36]. For this reason, the Chinese specification [44] prescribes a minimum embedded depth ratio of 3 for the CES columns.

Another parameter that has an impact on the seismic behavior of the CES column is the shear connector. On the CES composite specimens with steel shear connections, numerous analytical and experimental investigations have been carried out to examine the behavior of shear connectors under axial loads and combinations of axial and seismic loads. The findings demonstrated that, in comparison to non-seismic shear capacities, seismic loads cause a 40% decrease in the shear stud's capacity. This reduction happens as a result of seismic fatigue of the weld/connector materials and concrete crushing, which moves the stress distribution up the connector's shank and onto its head. This increases the connector's bending stresses and leads to earlier failures [12]. The shear stud capacity was unaffected by the studs' shear connectors' initial bending. Similar to static capabilities, the concrete strength had an impact on the seismic shear capacity of the studs [45]. As stiffness deterioration decreased, the columns with studs shown in Figure 13 demonstrated a greater capacity for deformation and energy dissipation.

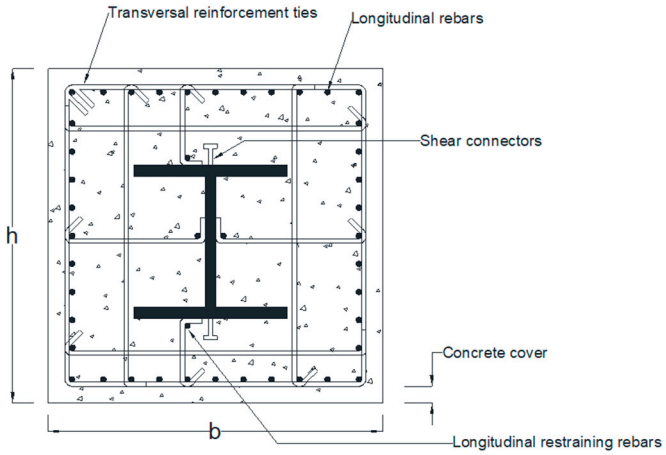

Figure 13. Cross section of CES column with shear connectors.

Many types and strengths of concrete have been used in composite buildings and substantial research in recent years. Concrete with a compressive strength greater than 50 MPa is referred to as high-strength concrete [46]. This type of concrete can be made with premium aggregates and superplasticizers, and its strength can even surpass 100 MPa. The cyclic behavior of CES columns with long webs of cross-shaped steel was more influenced by the concrete strength when the concrete strength rose, increasing the columns' shear capacity and a decrease in their ability to deform [47]. Additionally, as concrete strength

grew, so did the capacity of long CES columns [39]. The common failure modes of cyclically loaded high-strength CES columns, shear failure, shear–flexural failure, and flexural failure, are shown in Figure 14.

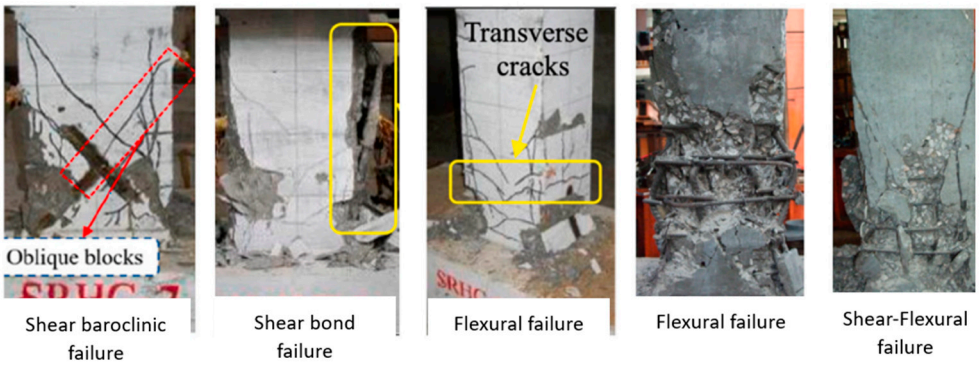

Figure 14. Typical failure mode of cyclically loaded high-strength CES column, reprinted with permission from [23], 2023, *Journal of Building Engineering*.

Based on the lateral displacement capacity of the column and its integration with the curvature distribution, the following equation for the length of the plastic hinge of the CES column is calculated and proposed [26]:

$$L_{rp} = (0.5d + 0.05h)\left\{(1 + 0.04t_{ek})\frac{M_m}{M_{y0}} - 0.25\right\} + 12(D_r - 12) \quad (16)$$

In Equation (16), the M_m is the maximal moment, M_{y0} is the yield moment, D_r is equal to the rebar diameter in mm, and t_{ek} is the ratio of A_s/A_r. Here, A_s is defined as the gross area of the steel section, and A_r is the gross area of the longitudinal rebars. Also, d is considered the effective column depth, and h is the column length. Figure 15 presents the plastic hinge length along the column height [26].

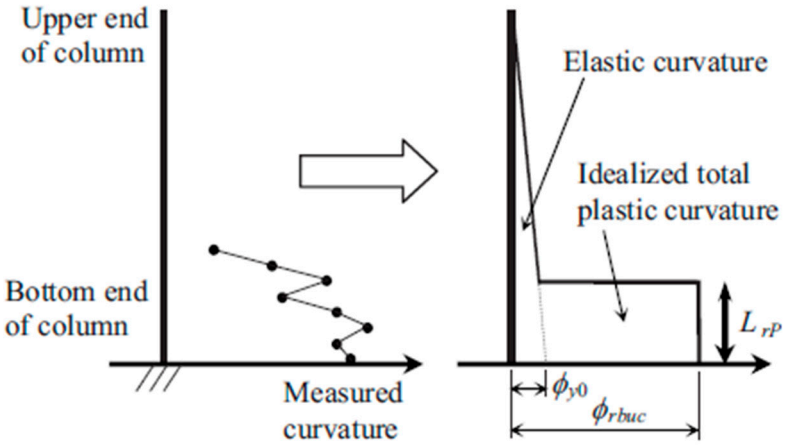

Figure 15. Plastic hinge length along the column, reprinted with permission from [26], 2010, *Journal of Bridge Engineering*.

When assessing seismic performance, the CES column's ductility is an essential metric. As seen in Figure 16, the ductility coefficient is essentially calculated as the ratio of lateral displacement corresponding to ultimate displacement and yield displacement, derived from the specimen's backbone curve. Generally speaking, excellent ductility is considered to be displayed by CES columns with a ductility coefficient greater than 3 [23].

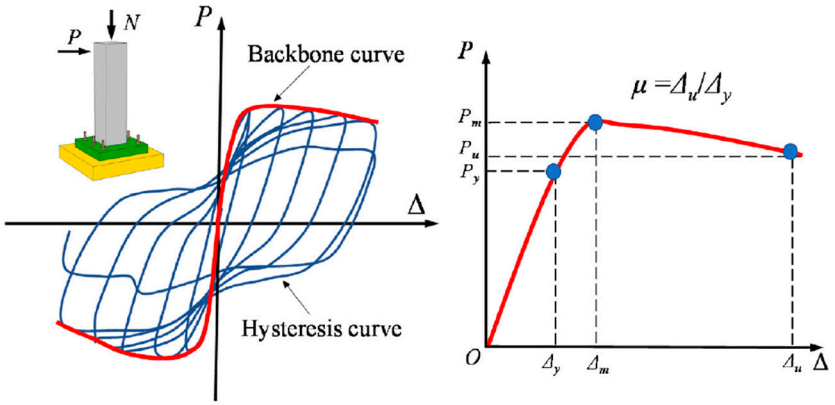

Figure 16. Ductility coefficient calculation on hysteresis curve, reprinted with permission from [23], 2023, *Journal of Building Engineering*.

Given the divergent perspectives, additional experimental research is required to elucidate the impact of steel sections at different load ratios.

Effect of Transverse Reinforcement on Behavior of Concrete-Encased Steel Columns

A large number of research works have been carried out in the past decade on the impact of transversal reinforcement on the behavior of the CES columns. The stirrup effectively confines the core concrete, and the seismic behavior of the CES compression-bending members is directly impacted by the stirrup spacing. It was found that as stirrup spacing increases, bearing capacity and ductility decrease [47]. Additionally, when the stirrup spacing increases from 75 to 100 mm, bearing capacity and ductility are reduced to a higher amount than when the spacing grows from 50 to 75 mm. This indicates that if the stirrup spacing stays below a particular threshold, it does not affect the ductility of CES columns. It suggests that the maximum stirrup spacing interval in the seismic area needs to be restricted. For this reason, the Chinese specification [44] suggests a value of 100 mm as the maximum spacing of stirrups for CES columns [47].

According to the experimental results, the CES column specimens' damage process usually includes the following: the deterioration of the concrete core; local buckling of the H-shaped steel flange; cracking on the buckled steel flange; longitudinal reinforcement bar buckling; and flexural cracks and spalling of the concrete cover at the base of the column. Figure 17 presents the rebar buckling caused by cyclic loading on the specimen of the CES column [26].

The confinement effect provided by stirrups is greatly reduced in short CES columns because the shear deformation allows for the stirrups to sustain a large amount of shear stress. As a result, the confinement stress acting on the concrete is reduced. Previous studies on confinement have shown that the stirrup's ability to confine can resist shear failure, keep the steel bar from buckling, and provide a pressure of confinement for the core concrete, all of which significantly increase the material's capacity and ductility. In addition, the stirrups serve to secure the longitudinal bars during construction and prevent them from buckling outward under pressure. This is particularly important for columns subjected to eccentric stresses, as it prevents spalling of the outer concrete cover, even at low load levels [12].

The stirrup ratio has a significant impact on how steel–concrete composite columns behave under seismic loads [36]. Increasing the stirrup ratio improves the seismic behavior, particularly when the axial compression ratio is high.

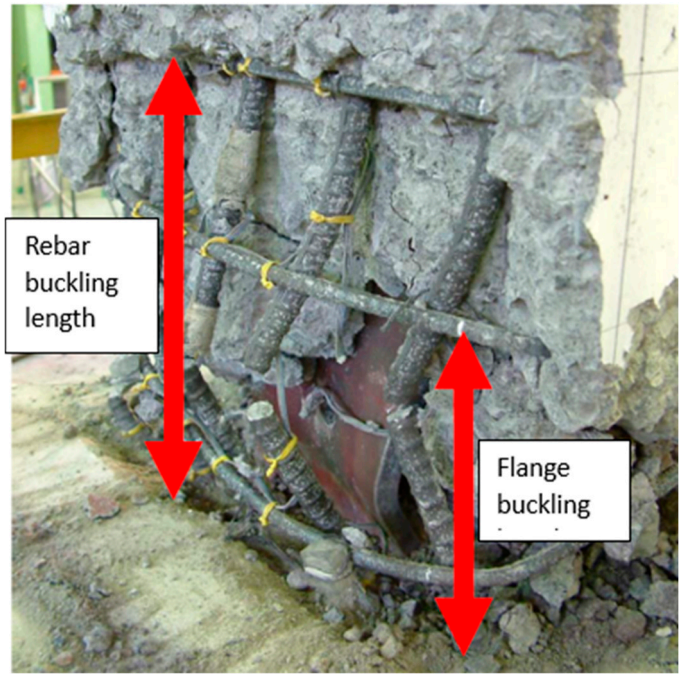

Figure 17. Damage to the column under cyclic loading, reprinted with permission from [26], 2010, *Journal of Bridge Engineering*.

6. Critical Views and Recommendations for Future Research

This study is a comprehensive compilation of information on several types of steel columns encased in concrete. A thorough literature review on various steel configurations for use in bridge applications has shown a lack of real-world project experience and a variety of current systems and tests.

In addition to emphasizing areas for development and improving construction techniques, this thorough review is essential for directing future research and promoting these technologies. CES technology opens the door for creative solutions in the industry and helps to navigate the difficulties of constructing bridges. A short list of the analytical parameters is provided, emphasizing how the analysis procedure uses them. The findings can be resumed as follows:

1. Fiber element modeling is a reliable method in order to represent the seismic behavior of the CES columns.
2. Confined concrete could be presented as highly confined concrete or partially confined concrete depending on the position of the concrete in the CES columns.
3. The length of the plastic hinge should be calculated for the CES column considering the presence of the steel profile embedded in the section as well as the rebar ratio.
4. The configuration of the transversal reinforcement also has an impact on the resistance of the CES columns.

Based on the model presented by [22], partially confined concrete could be modeled using the K_p coefficient factor and highly confined concrete could be modeled using the K_h coefficient factor in the CES column. However, based on the configuration and the shape of the steel section, these factors should be different.

The durability and seismic performance of concrete-encased steel bridge piers should be the main topics of future research. Evaluating these construction techniques' sustainability from an economic and environmental standpoint is essential. Additionally, research ought to focus on developing more robust designs, especially for areas with strong seismic activity.

It should be noted that the torsional behavior of the CES bridge piers has not been considered in this paper. There is very little research on the torsional behavior of the

CES columns in the buildings only [48]. Primarily, the torsional mode is not dominant in the seismic behavior of the bridges. However, in irregular or skewed bridges, the torsion effect could be more important. For this reason, future research should focus on the torsional behavior of the CES bridge piers as well as their impact on the seismic behavior of the bridge.

Future designs of concrete-encased steel columns will be greatly influenced by the analytical methodology discussed in this paper. Apart from the suggested configurations, the design parameters are also discussed. Bridges built with concrete-encased steel columns are more durable, leading to higher-quality structures.

7. Conclusions

This study discusses various analytical methods for concrete-encased steel columns. The configuration of the steel section and its seismic performance have been considered the primary subject of the current study since the seismic behavior of the CES columns is one of the most important factors in a successful design. Reviewing recent research, several facets of this issue are covered.

Even while CES columns have been the subject of numerous publications, manuals, and creative studies, there is still much room for more research on this topic. The requirements and needs of new projects might not be met by the commonly offered research studies, particularly in areas with high seismic demand. Developing and testing innovative steel and lateral reinforcement configurations for high seismic zones is one area that could use further improvement and investigation. There should be sufficient ductility and resistance in these CES portions to withstand seismic events.

Furthermore, considering the increasing emphasis on sustainability, future studies and implementations of innovative construction methods must prioritize environmental sustainability over structural soundness.

Author Contributions: Conceptualization, M.M. and M.H.; methodology, M.M. and M.H.; writing—original draft preparation, M.M.; writing—review and editing, M.H.; supervision, M.H. All authors have read and agreed to the published version of the manuscript.

Funding: This research received no external funding.

Institutional Review Board Statement: Not applicable.

Informed Consent Statement: Not applicable.

Data Availability Statement: No new data were created or analyzed in this study. Data sharing is not applicable to this article.

Conflicts of Interest: The authors declare no conflicts of interest.

References

1. American Institute of Steel Construction (AISC). Load and Resistance Factor Design of W-Shapes Encased in Concrete. 2003. Available online: https://www.aisc.org/globalassets/aisc/manual/15th-ed-ref-list/load-and-resistance-factor-design-of-w-shapes-encased-in-concrete.pdf (accessed on 15 June 2024).
2. Kartheek, T.; Venkat Das, T. 3D modelling and analysis of encased steel-concrete composite column using ABAQUS. *Mater. Today Proc.* **2020**, *27*, 1545–1554. [CrossRef]
3. Elbably, A.; Ramadan, O.; Akl, A.; Zenhom, N. Behavior of encased steel-high strength concrete columns against axial and cyclic loading. *J. Constr. Steel Res.* **2022**, *191*, 107161. [CrossRef]
4. Suresh Babu, S.; Priya; Rose Leema, A. State-of-the-Art Review for Concrete-Encased Steel Columns. 2020. Available online: https://rdcu.be/dD2eX (accessed on 15 June 2024).
5. Tian'e Longtan Bridge. Available online: https://www.highestbridges.com/wiki/index.php?title=Tian'e_Longtan_Bridge (accessed on 15 June 2024).
6. Zhang, Y.; Liu, Y.; Xin, H.; He, J. Numerical Parametric Study on Ultimate Load and Ductility of Concrete Encased Equal-leg Angle Steel Composite Columns. *Eng. Struct.* **2019**, *200*, 109679. [CrossRef]
7. Hybrid Hollow High Pier. 2018. 20 January 2019. Available online: http://www.actec.or.jp/3h_pier/pdf/3h_pier_pamphlet.pdf (accessed on 15 June 2024).

8. Paeglitis, A.; Gode, K. Concrete Bridge Deterioration Caused by De-Icing Salts in High Traffic Volume Road Environment in Latvia. *Balt. J. Road Bridge Eng.* **2014**, *9*, 200–207. [CrossRef]
9. Canadian Standards Association (CSA). *Canadian Highway Bridge Design Code*; CAN/CSA S6-14: Mississauga, ON, Canada, 2019.
10. *ACI Committee 318, Building Code Requirement for Reinforced Concrete (ACI 318-8) and Commentary (ACI 318R-8)*; American Concrete Institute: Farmington Hills, MI, USA, 2008.
11. *ANSI/AISC 360-16*; Specification for Structural Steel Buildings. American Institute of Steel Construction (AISC): Chicago, IL, USA, 2016.
12. Mostafa, M.A.; Wu, T.; Liu, X.; Fu, B. The Composite Steel Reinforced Concrete Column Under Axial and Seismic Loads: A Review. *Int. J. Steel Struct.* **2019**, *19*, 1969–1987. [CrossRef]
13. Spacone, E.; Filippou, F.C.; Taucer, F.F. Fiber beam–column model for non-linear analysis of R/C frames: Part I. Formulation. *Earthq. Eng. Struct. Dyn.* **1996**, *25*, 711–725. [CrossRef]
14. El-Tawil, S.; Deierlein, G.G. Nonlinear analysis of mixed steel–concrete frames. I: Element formulation. *J. Struct. Eng.* **2001**, *127*, 647–655. [CrossRef]
15. Kent, D.C.; Park, R. Flexural members with confined concrete. *J. Struct. Div.* **1971**, *97*, 1969–1990. [CrossRef]
16. Mander, J.B.; Priestley, M.J.; Park, R. Theoretical stress–strain model for confined concrete. *J. Struct. Eng.* **1988**, *114*, 1804–1826. [CrossRef]
17. Tan, E.L.; Thomas, C.; Siriviatnanon, V. Finite element modeling of nonlinear behaviour of headed stud shear connectors in foamed and lightweight aggregate concrete. In Proceedings of the Fifth International Conference on Advances in Experimental Structural Engineering (I), Taipei, Taiwan, 8–9 November 2013; Volumes 8 and 9.
18. Fang, L.; Zhang, B.; Jin, G.F.; Li, K.W.; Wang, Z.L. Seismic behavior of concrete-encased steel cross-shaped columns. *J. Constr. Steel Res.* **2015**, *109*, 24–33. [CrossRef]
19. Chen, S.; Wu, P. Analytical model for predicting axial compressive behavior of steel reinforced concrete column. *J. Constr. Steel Res.* **2017**, *128*, 649–660. [CrossRef]
20. Liang, C.Y.; Chen, C.; Weng, C.; Yin, Y.; Wang, J. Axial compressive behavior of square composite columns confined by multiple spirals. *J. Constr. Steel Res.* **2014**, *103*, 230–240. [CrossRef]
21. Mirza, S.A.; Skrabek, B. Statistical analysis of slender composite beam–column strength. *J. Struct. Eng.* **1992**, *118*, 1312–1332. [CrossRef]
22. Chen, C.C.; Lin, N.J. Analytical model for predicting axial capacity and behavior of concrete encased steel composite stub columns. *J. Constr. Steel Res.* **2006**, *62*, 424–433. [CrossRef]
23. Lai, B.; Bao, R.; Zhang, M.; Wang, Y.; Liew, J.Y. Evaluation on the static and seismic performance of steel reinforced concrete composite columns with high strength materials. *J. Build. Eng.* **2023**, *79*, 107886. [CrossRef]
24. Sheikh, S.A.; Uzumeri, S. Analytical model for concrete confinement in tied columns. *J. Struct. Div.* **1982**, *108*, 2703–2722. [CrossRef]
25. Cusson, D.; Paultre, P. Stress-strain model for confined high-strength concrete. *J. Struct. Eng.* **1995**, *121*, 468–477. [CrossRef]
26. Naito, H.; Akiyama, M.; Suzuki, M. Ductility Evaluation of Concrete-Encased Steel Bridge Piers Subjected to Lateral Cyclic Loading. *J. Bridge Eng.* **2011**, *16*, 72–81. [CrossRef]
27. Mirza, S.A.; Lacroix, E.A. Comparative Strength Analyses of Concrete-Encased Steel Composite Columns. *J. Struct. Eng.* **2004**, *130*, 1941–1953. [CrossRef]
28. Gautham, A.; Sahoo, D.R. Behavior of steel-reinforced composite concrete columns under combined axial and lateral cyclic loading. *J. Build. Eng.* **2021**, *39*, 102305. [CrossRef]
29. Xu, C.; Cao, P.Z.; Wu, K.; Lin, S.Q.; Yang, D.G. Experimental investigation of the behavior composite steel-concrete composite beams containing different amounts of steel fibres and conventional reinforcement. *Construct. Build. Mater.* **2019**, *202*, 23–36. [CrossRef]
30. Lai, B.; Richard Liew, J.Y.; Xiong, M. Experimental study on high strength concrete encased steel composite short columns. *Constr. Build. Mater.* **2019**, *228*, 116640. [CrossRef]
31. Lai, B.; Richard Liew, J.Y.; Venkateshwaran, A.; Li, S.; Xiong, M.J. Assessment of high-strength concrete encased steel composite columns subject to axial compression. *J. Constr. Steel Res.* **2020**, *164*, 105765. [CrossRef]
32. Ellobody, E.; Young, B. Numerical simulation of concrete encased steel composite columns. *J. Constr. Steel Res.* **2011**, *67*, 211–222. [CrossRef]
33. *AIJ-2014*; AIJ Standard for Structural Calculation of Steel Reinforced Concrete Structures. Architectural Institute of Japan: Tokyo, Japan, 2014. (In Japanese)
34. Lai, B.L.; Tan, W.K.; Feng, Q.T.; Venkateshwaran, A. Numerical parametric study on the uniaxial and biaxial compressive behavior of H-shaped steel reinforced concrete composite beam-columns. *Adv. Struct. Eng.* **2022**, *25*, 2641–2661. [CrossRef]
35. British Standard Institution. BS 5400-05: 1979: Steel, Concrete and Composite Bridges, Part 5, Code of Practice for Design of Composite Bridges. 2002. Available online: https://knowledge.bsigroup.com/products/steel-concrete-and-composite-bridges-code-of-practice-for-design-of-composite-bridges-1?version=standard&tab=preview (accessed on 15 June 2024).
36. Chen, C.; Wang, C.; Sun, H. Experimental Study on Seismic Behavior of Full Encased Steel-Concrete Composite Columns. *J. Struct. Eng.* **2014**, *140*, 04014024. [CrossRef]

37. Hassan, W.; Farag, M. Seismic performance of steel-reinforced concrete composite columns in existing and modern construction. *Soil Dyn. Earthq. Eng.* **2021**, *151*, 106945. [CrossRef]
38. Zhang, S.; Zhao, Z.; He, X. Flexural behavior of SRC columns under axial and bilateral loading. *Appl. Mech. Mater.* **2012**, *166–169*, 3383–3390. [CrossRef]
39. Yang, B.S.; Li, Y.Y. Study on the behaviors of steel reinforced concrete columns. *Adv. Mater. Res.* **2012**, *368–373*, 248–252. [CrossRef]
40. Dong, H.; Liang, X.; Cao, W. Seismic behavior of large-size encased cross-section steel-reinforced high-strength concrete circular columns. *Structures* **2021**, *34*, 1169–1184. [CrossRef]
41. Zhu, W.; Jia, J.; Gao, J.; Zhang, F. Experimental study on steel reinforced high-strength concrete columns under cyclic lateral force and constant axial load. *Eng. Struct.* **2016**, *125*, 191–204. [CrossRef]
42. Azizinamini, A.; Ghosh, S. Steel reinforced concrete structures in 1995 Hyogoken-Nanbu earthquake. *J. Struct. Eng.* **1997**, *123*, 986–992. [CrossRef]
43. Nagata, T.; Fukuchi, Y.; Wakamatsu, S. Experimental study on embedded depth and effective bearing flange width of steel members as bending: Strength of embedded type of steel reinforced concrete column base. In Proceedings of the Annual Meeting Architectural Institute of Japan, Tokyo, Japan, December 1999; Architectural Institute of Japan (AIJ): Tokyo, Japan; pp. 1167–1168.
44. Ministry of Housing and Urban-Rural Development of the People Republic of China. Code for Design of Composite Structures. JGJ 138-2016 (JGJ138-2010). Available online: https://www.chinesestandard.net/Related.aspx/JGJ138-2016 (accessed on 15 June 2024).
45. Civjan, S.A.; Singh, P. Behavior of shear studs subjected to fully reversed cyclic loading. *J. Struct. Eng.* **2003**, *129*, 1466–1474. [CrossRef]
46. Warner, R.; Rangan, B.; Hall, A.; Faulkes, K. *Concrete Structures*; Addison Wesley Longman: Boston, MA, USA, 1998.
47. Wang, Q.; Shi, Q.; Tao, Y. Experimental and numerical studies on the seismic behavior of steel reinforced concrete compression-bending members with new-type section steel. *Adv. Struct. Eng.* **2016**, *19*, 255–269. [CrossRef]
48. Zhou, C.; Xue, J.; Hu, Z.; Liu, Z. Coupled translational-torsional response for SRC frame with special-shaped columns under earthquake. *J. Build. Eng.* **2020**, *31*, 101440. [CrossRef]